Spatial separation of spoof surface acoustic waves on the graded groove grating

Han Jia, Minghui Lu, Xu Ni, Ming Bao, and Xiaodong Li

Articles you may be interested in

Guided propagation of surface acoustic waves and piezoelectric field enhancement in ZnO/GaAs systems
J. Appl. Phys. **110**, 103501 (2011); 10.1063/1.3660215

Strongly localized acoustic surface waves propagating along a V-groove
Appl. Phys. Lett. **94**, 023505 (2009); 10.1063/1.3072346

Implicit methods of solution to integral formulations in boundary element method based nearfield acoustic holography
J. Acoust. Soc. Am. **116**, 1559 (2004); 10.1121/1.1777854

Least action principle for the estimation of the slowness and the attenuation of pseudo surface acoustic waves
J. Appl. Phys. **93**, 10084 (2003); 10.1063/1.1574171

Transverse surface acoustic wave detection by scanning acoustic force microscopy
Appl. Phys. Lett. **73**, 882 (1998); 10.1063/1.122026

Spatial separation of spoof surface acoustic waves on the graded groove grating

Han Jia,[1] Minghui Lu,[2] Xu Ni,[2] Ming Bao,[1,a)] and Xiaodong Li[1]

[1]*Key Laboratory of Noise and Vibration Research, Institute of Acoustics, Chinese Academy of Sciences, Beijing 100190, China*
[2]*National Laboratory of Solid State Microstructures and College of Engineering and Applied Sciences, Nanjing University, Nanjing 210093, China*

In this paper, a rigid surface decorated with an array of grooves with graded widths is proposed to get spatial separation of the spoof surface acoustic waves. Because of the intermodal coupling between forward and backward modes on the graded structure, the spoof surface acoustic waves with different frequencies stop propagating ahead and reflect back at different positions of the graded groove grating. The intensity of acoustic field is effectively enhanced near the propagation-stop position due to the slow group velocity. We believe that such system with the capability of energy concentration and wave spatial arrangement by frequencies has potential applications in acoustic wave coupling and absorption. © 2014 AIP Publishing LLC.
[http://dx.doi.org/10.1063/1.4895990]

I. INTRODUCTION

The graded acoustic artificial structures, which have a gradual variation of their geometric parameters, play an important role in manipulating propagation of acoustic waves. By continuously changing either the lattice constant or the geometric size of the scatters, one can get phononic crystals or acoustic metamaterials with gradient index and realize many significant physical phenomena, such as acoustic focusing[1–6] and wave bending.[7] Besides bulk acoustic waves, focusing of Lamb waves in the elastic plate[8,9] has been also realized by introducing the graded structures.

Graded acoustic artificial structures can control not only the propagation directions of the waves but also the spatial distributions of the energy.[10,11] Recently, Zhu *et al.* designed a metamaterial, which consists of an array of grooves with graded depths perforated on a rigid plate, to control the acoustic energy spatial distribution.[11] They analyzed the acoustic dispersion relation on this graded structure by effective medium model and demonstrated the "rainbow trapping" effect, which has been widely investigated in optics.[12–16] Actually, the periodically textured rigid plate has attracted much research interest for the ability to support a new kind of surface acoustic waves (SAWs)—spoof SAWs (SSAWs) in recent years.[17–22] The SAWs on the periodically corrugated rigid surface originate from the coupling among the acoustic waves localized in the grooves. Therefore, the dispersion of SSAWs mainly depends on the geometrical parameters of the periodic structure rather than the material parameters. By exciting the SSAWs on the textured rigid plate, acoustic extraordinary transmission[17–19] and subwavelength imaging[20] have been realized. Focusing of SSAWs has also been realized through engraving gradient boreholes array in a rigid surface.[21] In this paper, we propose a rigid surface decorated with an array of grooves with graded widths to manipulate the spatial distribution of the SSAWs. The properties of SSAWs on this graded structure are analyzed by the finite element method (FEM). The numerical results show that the SSAWs with different frequencies stop propagating ahead and reflect back at different positions of the graded groove grating.

II. RESULTS AND DISCUSSION

The graded groove grating is schematically illustrated in Fig. 1(a). It consists of a one-dimensional (1D) air grooves array engraved in the surface of a rigid plate. The period (a) and the depth (h) of the unit groove, as shown in Fig. 1(b), are fixed at $a = 20$ mm and $h = 20$ mm, respectively. The whole grating has 46 grooves with gradient widths (w) from 3.0 mm to 7.5 mm. The change of the groove width is linear and the increment is $\Delta w = 0.1$ mm.

Before discussing the SSAWs on the graded groove grating, the dispersion relations of the SSAWs on the uniform groove gratings with different constant groove widths were calculated by FEM and shown in Fig. 2(a). It can be observed that all the SSAWs dispersion curves emanate from the air dispersion line. These dispersion curves run farther away from the air dispersion line and flatten out as the wave vector increasing. When reaching the boundary of the Brillouin zone, the SSAWs dispersion curves are almost
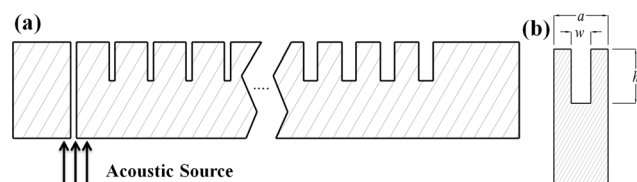

FIG. 1. (a) Schematic illustration of the groove grating with graded groove widths. (b) Unit cell of the graded groove grating in (a).

a)Author to whom correspondence should be addressed. Electronic mail: baoming@mail.ioa.ac.cn.
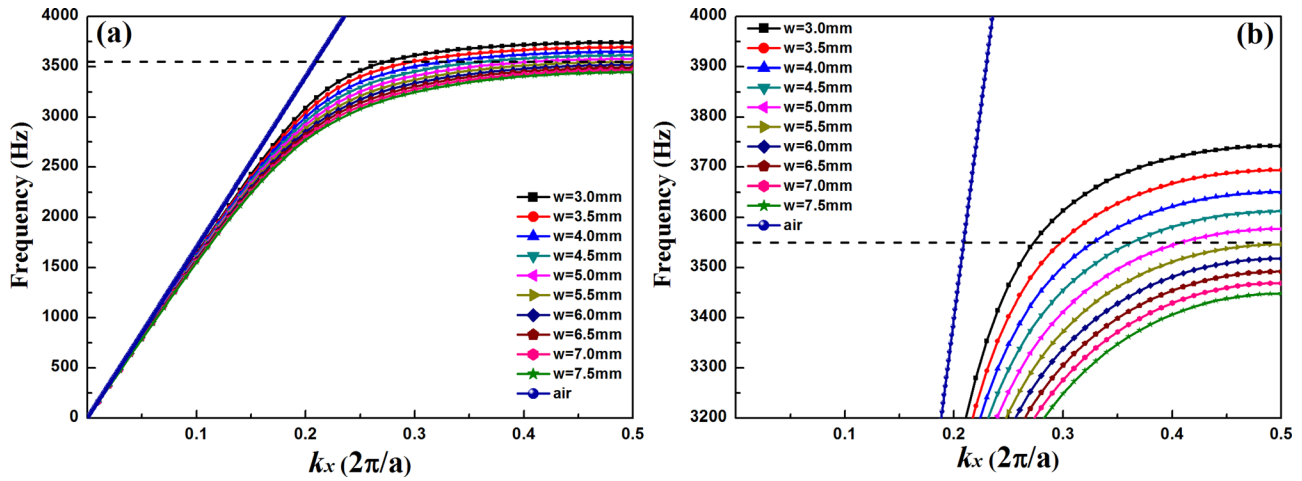
FIG. 2. (a) Dispersion curves of the SSAWs for the uniform groove array with different groove widths. Both the groove period and the groove depth are fixed at 20 mm. (b) A close-up of the dispersion curves in (a) around the band edge. The horizontal black dashed line indicates the frequency of 3550 Hz.

horizontal, which signifies nearly zero group velocity of SSAWs, since $v_g = \frac{\partial \omega}{\partial k}$.

Though these SSAWs dispersion curves have similar shapes, the cutoff frequencies vary with the change of the groove width, which can be observed more clearly from the dispersion curves zoomed in near the band edge in Fig. 2(b). From the previous research,[22] we know that SSAWs originate from the coupling among the acoustic waves localized in the periodical grooves. The coupling strength between the localized acoustic waves in adjacent grooves significantly affects the properties of the SSAWs. In the small groove width case, the distance between the grooves is large and the coupling is weak, so the dispersion curve of the SSAWs is prone to keep the form of the individual resonance. When the groove width increases, the coupling becomes more intensive with the decreasing distance between the grooves. And the dispersion curve of the SSAWs runs farther away from both the cavity resonance frequency and the air dispersion line. Therefore, the dispersion curve for the groove grating with larger groove width is below that with smaller groove width and the cutoff frequency decreases as the groove width increases.

Then, we turn to the SSAWs on the grating with graded groove widths as shown in Fig. 1(a). Because the width increment between the adjacent grooves is small, we could regard every single groove in the graded grating as a cell of a uniform groove grating, and the SSAWs on this single groove are inclined to present similar characteristics to those on the corresponding uniform groove grating. So the SSAWs will present different properties at different positions of the graded groove grating. In our system, the width of the groove increases linearly from the left-hand side ($w = 3.0$ mm) to the right-hand side ($w = 7.5$ mm), so the corresponding SSAWs dispersion curve descends monotonically. The dispersion curves in Fig. 2(b) show that the cutoff frequencies decrease from 3743 Hz to 3448 Hz. This variation of the SSAWs dispersion characteristics with the position will give rise to very different propagation property from that on a uniform groove grating. When the SSAWs with frequency of 3550 Hz, which lies in the cutoff frequency range and is

indicated by the horizontal dashed line in Fig. 2, are induced at the left-hand side of the graded groove grating, the excited mode locates at the intersection of the horizontal dashed line and the black curve (the dispersion curve for the uniform groove grating with groove width $w = 3.0$ mm). As the SSAWs propagating towards the right-hand side, the mode transfers from left dispersion curve to the right one. Because the whole energy of SSAWs exists in air, the wave vector should satisfy the formula

$$k_x^2 + k_z^2 = k_a^2,$$

where k_x and k_z are the horizontal component and the vertical component of the SSAWs vector and k_a is the bulk wave vector in air. For SSAWs, the horizontal component of the wave vector is larger than bulk wave vector in air, i.e., $k_x > k_a$, wherefore the vertical component (k_z) is purely imaginary, which represents the attenuation speed in the vertical direction. The increase of the wave vector in propagation direction results in the larger imaginary part in the attenuation direction, which indicates quicker attenuation speed and stronger localization. In Fig. 2, one can also observe that the slope of the dispersion curve at the intersection decreases as the wave vector increases and reaches nearly zero when the wave vector approaches the boundary of the Brillouin zone. Hence, as propagating from left-hand side to right in our system, the SSAWs will localize more tightly at the textured surface and the group velocity will decrease gradually. When the SSAWs arrive at the groove where the corresponding cutoff frequency is 3550 Hz, the group speed reduces to zero and the SSAWs stop propagating ahead. This extremely slow propagation speed and the highly localization could result in the intensity enhancement.

Next, we calculated the field distributions for the SSAWs with different frequencies in frequency domain by FEM. The simulated system is the same as that schematically illustrated in Fig. 1(a). A slit with 3 mm width is drilled on the left of the grooves array. The center-to-center distance between the slit and the leftmost groove is 20 mm. The center of the leftmost groove surface is set as the origin of the
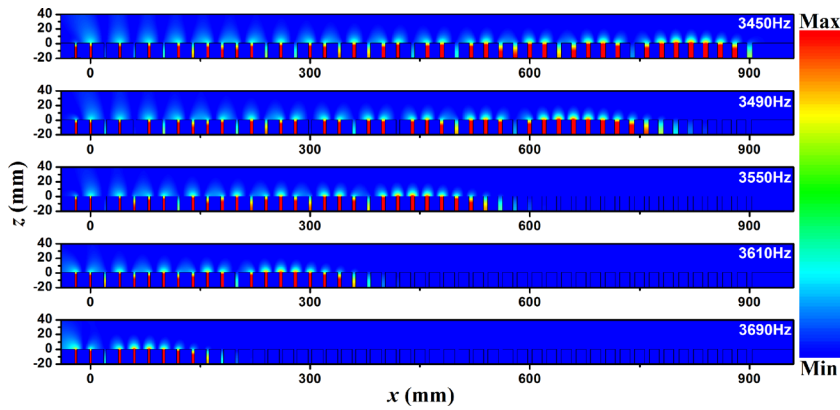
FIG. 3. Normalized acoustic amplitude distributions for five different frequencies within the cutoff frequency range. The frequency is indicated in each panel. Each distribution is normalized by the maximum pressure value above the textured surface.

coordinates. An acoustic source is placed below the slit. Because the width of the slit is far smaller than the operation wavelength, the SSAWs can be effectively excited by the waves coming out from the slit. The simulated acoustic pressure amplitude distributions for five different frequencies within the cutoff frequency range are shown in Fig. 3. All these acoustic distributions are normalized by the maximum amplitude values above the textured surface. It is observed that the SSAWs are successfully excited for all these frequencies and propagate towards right-hand side. The tails of the energy distribution in the vertical direction become shorter as propagating, which indicates that the localization is more intensive. The SSAWs with different frequencies finally stop propagating ahead and reach maximum amplitude at different positions of the graded groove grating. The properties of the acoustic amplitude distributions in Fig. 3 coincide well with the prediction in dispersion analysis.

To clearly understand the acoustic characteristics, the amplitude distributions along the line 2 mm above the surface were extracted and shown in Fig. 4. Though the SSAWs with different frequencies stop propagating at different positions, their amplitude distributions exhibit similar oscillations. The short-scale oscillations correspond to the Bloch modes introduced by the periodical structures. And the peaks

of these short-scale oscillations, especially near the propagation-stop position, also exhibit oscillated form (illustrated by the dashed lines). These long-scale oscillations are attributed to the coupling between the forward and backward SSAWs: the incident acoustic energy carried by the forward mode couples to the backward mode during the propagation; the backward mode and the forward mode interfere with each other and form the standing-wave pattern, i.e., the long-scale oscillations. This coupling strengthens as the wave vector approaches the boundary of the Brillouin zone. At last, all energy of the SSAWs is reflected back but trapped around the propagation-stop position. The propagation of SSAWs on this graded groove grating resembles a rigid ball bumping into an elastic-soft wall, slowing down gradually, and then bouncing back.

In Fig. 5, the acoustic amplitude distributions 2 mm above the textured surface for more detailed frequencies in cutoff frequency range are plotted as a color map. Different from those in Fig. 4, all the acoustic amplitude distributions here are normalized by the acoustic amplitude at the slit center ($x = -20$ mm), i.e., entrance of the acoustic waves. So the colors in Fig. 5 represent the amplitude amplification factors during the propagating—the upper color in the color bar corresponding to a larger amplification factor. Despite the spatial oscillation along the horizontal axis, the amplification factor also oscillates with the variation of the frequency. We
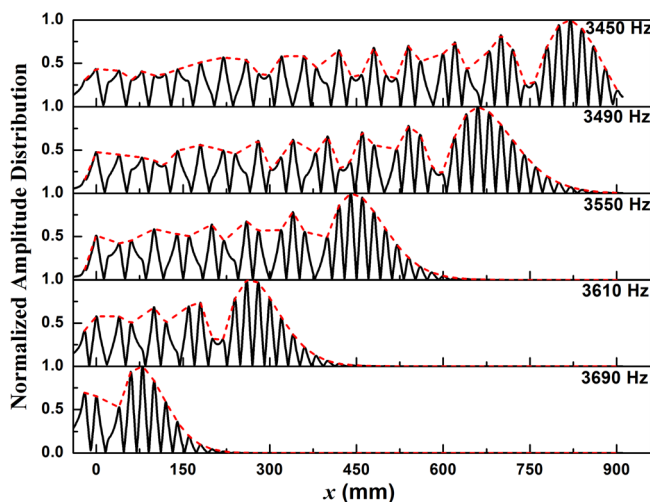

FIG. 4. Normalized acoustic amplitude distribution lines (black solid lines) 2 mm above the graded textured surface for the same frequencies in Fig. 3. The peaks of the distribution oscillations are connected by the red dashed lines.
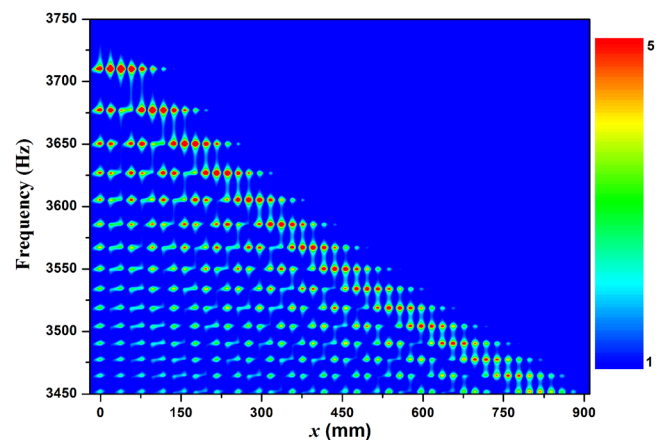

FIG. 5. Color map for normalized acoustic amplitude distributions 2 mm above the graded textured surface within the cutoff frequency range. All the acoustic amplitude distributions are normalized by the acoustic amplitude at the entrance of the acoustic waves ($x = -20$ mm).

attribute this oscillation to the formation of the standing-waves of SSAWs. In finite system, there always exist some discrete standing-wave modes that can be effectively excited. There are two boundaries in our system: the slit entrance and the boundary at the propagation-stop position. So only the SSAWs with the frequencies, which are supported in this finite system, can be excited intensely.

III. CONCLUSION

In conclusion, we have proposed a rigid surface decorated with an array of grooves with graded widths to slow down the SSAWs. Because of the intermodal coupling between forward and backward modes, the acoustic energy with different frequencies is reflected back at different positions. The intensity of acoustic field is effectively enhanced near the propagation-stop position due to the slow group velocity. Compared to the graded grating with varying groove depth,[11] our planar system is easier to implant into the acoustic devices. We believe that the proposed system has potential applications in acoustic wave coupling and absorption.

ACKNOWLEDGMENTS

[1]T. P. Martin, M. Nicholas, G. J. Orris, L. W. Cai, D. Torrent, and J. Sánchez-Dehesa, Appl. Phys. Lett. **97**, 113503 (2010).

[2]S. Peng, Z. He, H. Jia, A. Zhang, C. Qiu, M. Ke, and Z. Liu, Appl. Phys. Lett. **96**, 263502 (2010).

[3]Y. Li, B. Liang, X. Tao, X. F. Zhu, X. Y. Zou, and J. C. Cheng, Appl. Phys. Lett. **101**, 233508 (2012).

[4]L. Zigoneanu, B. I. Popa, and S. A. Cummer, Phys. Rev. B **84**, 024305 (2011).

[5]S. C. S. Lin, T. J. Huang, J. H. Sun, and T. T. Wu, Phys. Rev. B **79**, 094302 (2009).

[6]A. Climente, D. Torrent, and J. Sánchez-Dehesa, Appl. Phys. Lett. **97**, 104103 (2010).

[7]L. Y. Wu and L. W. Chen, J. Appl. Phys. **110**, 114507 (2011).

[8]J. Zhao, R. Marchal, B. Bonello, and O. Boyko, Appl. Phys. Lett. **101**, 261905 (2012).

[9]T. T. Wu, Y. T. Chen, J. H. Sun, S. C. S. Lin, and T. J. Huang, Appl. Phys. Lett. **98**, 171911 (2011).

[10]V. Romero-García, R. Picó, A. Cebrecos, V. J. Sánchez-Morcillo, and K. Staliunas, Appl. Phys. Lett. **102**, 091906 (2013).

[11]J. Zhu, Y. Chen, X. Zhu, F. J. Garcia-Vidal, X. Yin, W. Zhang, and X. Zhang, Sci. Rep. **3**, 1728 (2013).

[12]K. L. Tsakmakidis, A. D. Boardman, and O. Hess, Nature **450**, 397 (2007).

[13]Q. Gan, Z. Fu, Y. J. Ding, and F. J. Bartoli, Phys. Rev. Lett. **100**, 256803 (2008).

[14]Q. Gan, Y. J. Ding, and F. J. Bartoli, Phys. Rev. Lett. **102**, 056801 (2009).

[15]Q. Gan, Y. Gao, K. Wagner, D. Vezenov, Y. J. Ding, and F. J. Bartoli, Proc. Natl. Acad. Sci. U. S. A. **108**, 5169 (2011).

[16]S. He, Y. He, and Y. Jin, Sci. Rep. **2**, 583 (2012).

[17]J. Christensen, A. I. Fernandez-Dominguez, F. de Leon-Perez, L. Martin-Moreno, and F. J. Garcia-Vidal, Nat. Phys. **3**, 851 (2007).

[18]J. Christensen, L. Martín-Moreno, and F. J. García-Vidal, Phys. Rev. B **81**, 174104 (2010).

[19]Y. Zhou, M. H. Lu, L. Feng, X. Ni, Y. F. Chen, Y. Y. Zhu, S. N. Zhu, and N. B. Ming, Phys. Rev. Lett. **104**, 164301 (2010).

[20]H. Jia, M. Lu, Q. Wang, M. Bao, and X. Li, Appl. Phys. Lett. **103**, 103505 (2013).

[21]Y. Ye, M. Ke, Y. Li, T. Wang, and Z. Liu, J. Appl. Phys. **114**, 154504 (2013).

[22]Z. He, H. Jia, C. Qiu, Y. Ye, R. Hao, M. Ke, and Z. Liu, Phys. Rev. B **83**, 132101 (2011).